Article

Modeling Investigation of Brown Carbon Aerosol and Its Light Absorption in China

Yong Zhu [1,2]**, Qiaoqiao Wang** [1,2,*]**, Xiajie Yang** [1,2]**, Ning Yang** [1,2] **and Xurong Wang** [1,2]

1. Institute for Environmental and Climate Research, Jinan University, Guangzhou 511443, China; zhuyong@stu2018.jnu.edu.cn (Y.Z.); jnuyxj2019@stu2019.jnu.edu.cn (X.Y.); yangn@stu2020.jnu.edu.cn (N.Y.); xurong@stu2018.jnu.edu.cn (X.W.)
2. Guangdong-Hongkong-Macau Joint Laboratory of Collaborative Innovation for Environmental Quality, Guangzhou 511443, China
* Correspondence: qwang@jnu.edu.cn

Abstract: Brown carbon (BrC) is a type of organic carbon with light-absorbing abilities, especially in ultraviolet (UV) radiation, which could significantly contribute to global warming. Observations have shown high BrC concentrations and absorption in China, suggesting potentially large BrC emissions. The potential contribution of fossil fuel combustion to BrC emission has been ignored in most previous studies. Here, we use GEOS-Chem to simulate BrC distribution and absorption in China, accounting for three major primary BrC sources: residential coal and biofuel combustion, vehicle exhausts, and open biomass burning. Based on the literature and related energy consumption data, we estimate the specific emission ratio of BrC versus BC, and BrC mass absorption efficiency (MAE) for each source. Combined with BC emission, total BrC emission in China is then estimated to be 3.42 Tg yr^{-1} in 2018, of which 71% is from residential combustion, 14% is from vehicle exhaust, and 15% is from open biomass burning. Residential combustion is the main source of surface BrC in China, accounting for 60% on average, followed by open biomass burning (23%) and vehicle exhaust emissions (17%). There is a clear seasonality in surface BrC concentrations with the maximum in winter (5.1 µg m^{-3}), followed by spring (2.8 µg m^{-3}), autumn (2.3 µg m^{-3}), and summer (1.3 µg m^{-3}). BrC AAOD at 365 nm ranges from 0.0017 to 0.060 in China, mainly dominated by residential combustion (73%), followed by open biomass burning (16%), and vehicle exhaust emissions (11%). It is also estimated that BrC accounts for 45–67% (52% on average) of total carbonaceous aerosol AAOD at 365 nm, implying an equal importance of BrC and BC regarding the absorption in UV radiation.

Keywords: brown carbon (BrC); AAOD; residential combustion; coal combustion; vehicle exhaust; biomass burning

1. Introduction

Brown carbon (BrC) is a type of organic matter that absorbs light in the visible to ultraviolet (UV) ranges with a strong wavelength dependence and a significant enhancement of light absorption towards the UV regions [1–3]. In highly polluted areas, BrC can dominate the light absorption of aerosols, and results in a regional direct radiative forcing of up to 3–4 W m^{-2} [4]. Accounting for BrC warming effect can even change the regional direct radiative forcing of organic carbon (OC) aerosols from cooling effect (without considering BrC) to warming effect [5,6]. On the global scale, the warming effect of BrC can reach 30–70% of black carbon (BC) and 15–40% of CO_2 [7]. BrC can also affect the formation, the microphysical properties, and the lifetime of clouds, either by acting as cloud condensation nuclei and ice nuclei or through heating the cloud layer [8–11]. Therefore, BrC plays a key role in regional and global aerosol climate effect.

Observations have shown that BrC surface concentrations in China are generally higher than those observed in European countries [12–14]. For example, Wang et al. (2013) reported a BrC column burden of 40–90.5 mg m^{-2} in Winter, Beijing, much higher than

the global average burden of 0.65 mg m^{-2} [5,15]. In addition to the high pollution level, BrC in China also has a relatively stronger light absorption ability. For instance, the mass absorption efficiency at wavelength of 365 nm (MAE$_{365}$) of water-soluble brown carbon in Beijing is around 0.7–1.8 m^2 g^{-1}, which is significantly higher than that in the southeastern United States (0.3–0.7 m^2 g^{-1}) [16,17]. Studies have also reported much higher absorption coefficients in Beijing (3.7–10 Mm^{-1}) and Sanjiang Plain (22 $\pm$ 36 Mm^{-1}) in China than those in the United States (0.40–0.88 Mm^{-1}), Central and Southern Europe (1.1–4.7 Mm^{-1}), and South Korea (2.7 $\pm$ 1.4 Mm^{-1}) [12,18–21]. The high BrC level, combined with high MAE and the consequently high absorption coefficients, indicate a potentially significant climate effect of BrC in China.

There are various sources of BrC in the atmosphere, including incomplete combustion of biomass and fossil fuel, as well as secondary formation [2,5,20,22,23]. Biomass burning is recognized as the most important source of BrC on a global scale [2,4,24]. The potential contribution of fossil fuel combustion to BrC emissions has been pointed out recently. For instance, Xie et al. (2017) [23] and Du et al. (2014) [18] reported that vehicle exhausts contain a large amount of BrC. In addition, Sun et al. (2017) [25] reported about 592 Gg BrC (compared with 482 Gg BC) emitted from residential coal combustion.

Due to the lack of an emission inventory of BrC, most previous model studies either neglect BrC or simply equate BrC with the OC emitted from biomass burning [26,27]. However, recent studies have pointed out that fossil fuel combustion could be a large BrC source, especially in China, due to the huge amount of energy consumption [23,25,28]. Besides this, the optical properties of BrC vary largely with sources [2]. Therefore, it is necessary to consider all potential sources of BrC as well as the corresponding optical properties for each source to improve the understanding of the climate effects due to BrC.

In this study, we use a chemical transport model GEOS-Chem to simulate BrC distribution and its light absorption in China. By considering the emissions from residential coal and biofuel combustion, vehicle exhaust, and open biomass burning combined with the corresponding optical properties for each source, the study aims to (1) investigate the pollution level of BrC in China and (2) improve the estimate of light absorption due to BrC compared with BC in China.

2. Model Description

We used a chemical transport model GEOS-Chem (version 12.0, http://geos-chem.org, accessed on 2 May 2021) to simulate BrC distribution and its absorption in China. The GEOS-Chem uses assimilated meteorological data GEOS-FP from NASA Global Modeling and Assimilation Office (GMAO) [29]. GEOS-FP data have an original horizontal resolution of 0.25$°$ $\times$ 0.3125$°$ and 72 vertical layers, with a top layer of around 0.01 hPa. In order to save computational resources, we reduced the number of vertical layers to 47, mainly by merging layers in the stratosphere. The simulation was performed with a nested domain over China with a horizontal resolution of 0.25$°$ $\times$ 0.3125$°$. The boundary conditions for the nested simulation were from the global simulation, with a horizontal resolution of 2$°$ $\times$ 2.5$°$.

The simulation was conducted for the year of 2018 with a full-chemistry simulation of NO$_x$-O$_x$-Hydrocarbon-aerosol. Simulated aerosols include SO$_4^{2-}$, NO$_3^-$, NH$_4^+$, carbonaceous aerosols (including BC and OC), dust, and sea salt. The simulation of carbonaceous aerosols in GEOS-Chem, as described by Park et al. (2003) [30], accounted for all the atmospheric processes (i.e., emissions, transport, diffusion, aging, secondary formation of OC, and dry and wet deposition). It was assumed that 80% of BC and 50% of primary OC were emitted as hydrophobic, and then became hydrophilic, with an e-folding time of 1.15 days.

2.1. Emissions

For the base simulation, the emissions from anthropogenic sources were from the Multi-resolution Emission Inventory for China (MEIC), based on the year of 2017 (http:

//meicmodel.org/?page_id=89, accessed on 2 May 2021). The inventory includes emissions from agriculture, power plants, industry, residential, and transportation sources. The open biomass burning emissions were from the Global Fire Emissions Database (QFED) v2.4r6, with a time resolution of 1 day [31]. Total BC emissions in China are 1.3 Tg yr^{-1}, of which 49% is from residential combustion, 23% is from vehicle exhaust, and 4.1% is from open biomass burning. The residential combustion mainly refers to coal and biofuel combustion in household stoves. In order to isolate the contribution of residential combustion, vehicle exhaust, and open biomass burning, a series of sensitivity tests were performed in addition to the base simulation, with each test having one of the above emission sources turned off (see Table 1). The difference between the base simulation and each sensitivity test could thus be attributed to the contribution of the specific emission source.

Table 1. Emissions used in different simulations.

Tests	Emissions
Base	Default
Case 1	Without residential combustion
Case 2	Without vehicle exhaust
Case 3	Without open biomass burning

2.2. Treatment of Brown Carbon

Most of the previous model studies either neglect BrC or simply use OC from biomass burning as a proxy of BrC. In this study, we consider three major primary sources of BrC: residential combustion (including coal and biofuel), vehicle exhaust, and open biomass burning, which are currently reported as being potentially large BrC sources [23,28,32]. Due to the lack of emission inventories, the emissions of BrC awee estimated based on the emission ratios of BrC versus BC ($E_{BrC/BC}$) combined with BC emissions for different sources. Assuming that the atmospheric process of BrC is similar to BC, the atmospheric concentrations of BrC emitted from each source could be estimated as the product of the corresponding $E_{BrC/BC}$ and BC concentrations, as the simulation of BC in GEOS-Chem is linear (i.e., concentrations are proportional to emissions). The calculation of total BrC concentrations can then be described by Equation (1):

$$C_{BrC} = \sum_i c_i \cdot E_{Brc/BC,i} \tag{1}$$

where C_{BrC} is total mass concentration of BrC, μgC m^{-3}; i represents a certain type of emission sources, c_i is the BC mass concentration emitted from source i, and $E_{Brc/BC,i}$ is the emission ratio of BrC versus BC for source i.

The corresponding $E_{Brc/BC}$ for each source used in the study are listed in Table 2. For residential combustion, we first decided on $E_{Brc/BC}$ for residential coal combustion and residential biofuel combustion, respectively, and then obtained the mean value weighted by BC emissions from each source. We used $E_{BrC/BC}$ of 5.9 for biofuel combustion based on the study of Sun et al. (2021) [32] and calculated $E_{BrC/BC}$ for coal combustion based on the usage of bituminous coal chunks, bituminous coal briquettes, anthracite coal chunks, and anthracite coal briquettes combined, with the corresponding $E_{BrC/BC}$ for each coal type adopted from Sun et al. (2017) [25]. Finally, based on BC emissions of 547 Gg yr^{-1} from residential coal combustion and 435 Gg yr^{-1} from residential biofuel combustion adopted from Wang et al. (2012) [33], we derived an $E_{BrC/BC}$ of 3.9 for residential combustion. $E_{BrC/BC}$ for open biomass burning (9.9) and vehicle exhaust (1.7) were adopted from the study of Tang et al. (2020) [34].

Table 2. $E_{BrC/BC}$ and emissions of BrC as well as the corresponding MAE at wavelength of 365 nm from different sources.

Sources	MAE (m^2 gC^{-1})	$E_{BrC/BC}$	Emissions (Tg yr^{-1})
Residential combustion	2.1	3.9	2.42
Vehicle exhaust	0.74	1.7	0.49
Open biomass burning	2.3	9.9	0.51

The absorbing aerosol optical depth (AAOD) due to BrC could be described by Equation (2):

$$AAOD_{BrC} = \sum_i m_i \cdot MAE_i \tag{2}$$

where m_i is the BrC column burden emitted from source i, gC m^{-2}; MAE_i represents the mass absorption efficiency of BrC emitted from source i, m^2 gC^{-1}. The BrC MAE for each source at a wavelength of 365 nm is also listed in Table 2. Similar to $E_{Brc/BC}$, the MAE for residential combustion is a weighted average of those for residential coal combustion and residential biofuel combustion. We used an MAE of 2.3 for biofuel combustion based on the study of Tang et al. (2020) [34] and calculated the MAE for coal combustion based on the usage of bituminous coal, anthracite coal, combined with the corresponding MAE for each coal type adopted from Li et al. (2019) [35], Tang et al. (2020) [34] and Wang et al. (2020) [36]. The MAE derived for residential combustion was 2.1 m^2 gC^{-1}. The MAE for vehicle exhaust (0.74 m^2 gC^{-1}) is the average from the study of Tang et al. (2020) [34] and Du et al. (2014) [18], while the MAE for open biomass burning (2.3 m^2 gC^{-1}) was adopted from the study of Tang et al. (2020) [34]. Pani et al. (2021) [37] reported a mean MAE of 2.4 ± 0.3 m^2 g^{-1} at 370 nm for biomass burning BrC, consistent with the value used in our study. Zhang et al. (2021) [38] also used an MAE of 4.1 m^2 g^{-1} and 0.886 m^2 g^{-1} at 350 nm and 550 nm, respectively, for biomass burning BrC in their model simulation. In addition, we used MAE values (at 365 nm) of 10 m^2 g^{-1} for BC [39] and 0.087 m^2 g^{-1} for dust [40] for the estimates of AAOD of carbonaceous and total aerosol.

3. Results

3.1. BrC Emissions in China

The total estimated emission of BrC in China in 2018 is 3.42 Tg yr^{-1}, of which 71% is from residential combustion, 14% is from vehicle exhaust, and 15% is from open biomass burning (Table 2). Emissions from residential combustion are the highest in winter, especially in January, with a maximum of 0.45 Tg month^{-1}, but start to decrease in spring. In contrast, emissions from open biomass burning peak in spring, with a maximum of 0.11 Tg month^{-1} in April. There are no obvious seasonal changes in vehicle exhaust emissions. Figure 1 shows the spatial distribution of BrC emissions in China during the year 2018 from residential combustion, vehicle exhaust, and open biomass burning. BrC emissions from residential combustion concentrated in Central, North and Northeast China. BrC emissions from vehicle exhaust are relatively higher in the North China Plain, Yangtze River Delta and Pearl River Delta, with hotspots in megacities. In contrast, the emissions from open biomass burning are scattered and are relatively higher in Northeast Plain.

3.2. Surface Concentrations in China

Figure 2 shows the simulated spatial distribution of annual mean surface BrC concentrations in 2018. The annual mean concentrations of BrC in China range from 0.050 to 20 μg m^{-3}, with an average of 2.9 μg m^{-3}, The spatial distribution of surface BrC concentrations is similar to the pattern of BrC emissions, with much higher concentrations in East and Central China than in West China. The hotspots in the Northeast Plain, North China Plain, Sichuan Basin, and Hubei province are apparent in Figure 2 and are mainly dominated by residential combustion. The regions with the lowest BrC concentrations

are found in Western China and Inner Mongolia, where population density and economic levels are low.
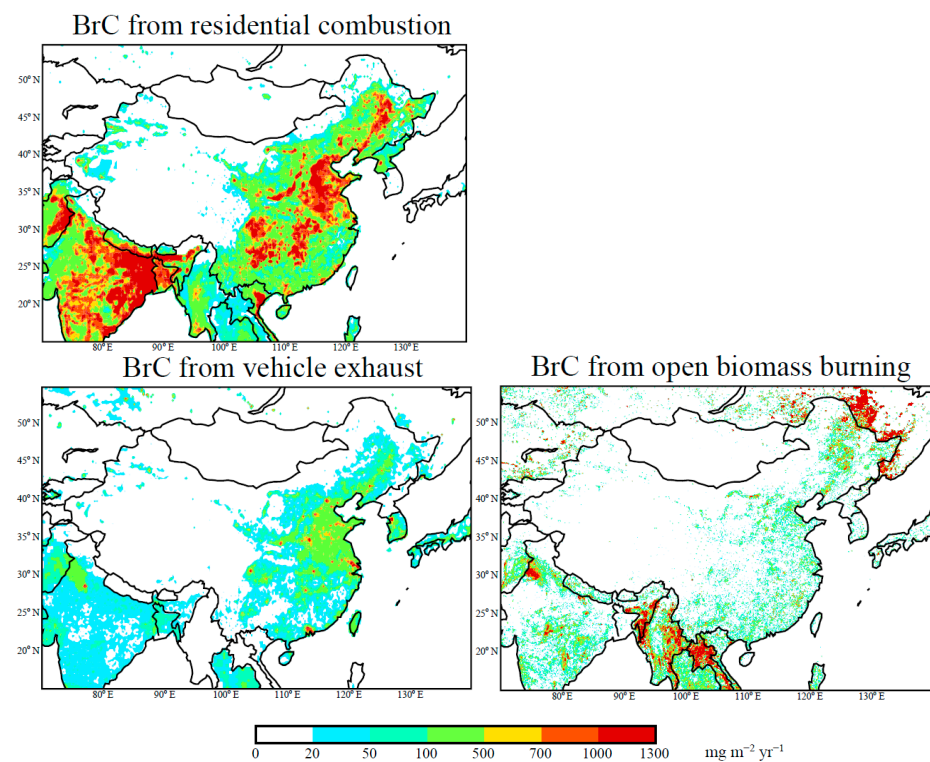

Figure 1. GEOS-Chem emissions of BrC from residential combustion, vehicle exhaust, and open biomass burning in 2018 in China.
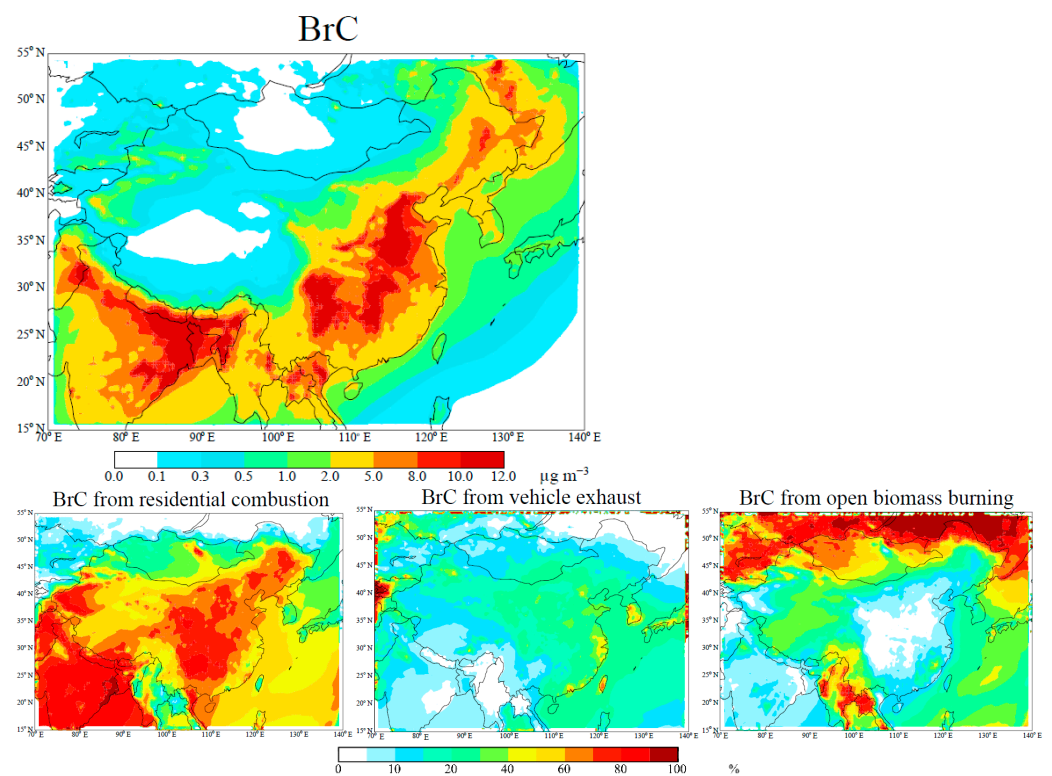

Figure 2. Simulated annual mean surface concentrations of BrC as well as the relative contribution from the specific source, i.e., residential combustion, vehicle exhaust, and open biomass burning.

Compared with other sources, residential combustion is the main source of BrC in China, accounting for 60% of total surface BrC concentrations in China. This result could be explained by the wide usage of biofuel and coal for cooking and heating, especially in rural regions, combined with high BrC emissions due to low combustion efficiency and little emission control. High contributions (>70%) are generally found in Central China. Vehicle exhaust accounts for 17% of surface BrC on average, with relatively higher contributions found in Beijing, Yangtze River Delta, and Pearl River Delta (>40%). Open biomass burning accounts for 23% of surface BrC on average, with maximums on the northeastern and southwestern border of China (40–90%), probably due to biomass burning in neighboring countries. There is also relatively high open biomass burning contribution in Fujian province, reaching up to 50%. This is consistent with previous studies, which show abundant BrC aerosols transported from Southeast Asia (e.g., Indochina) to southern China, especially in spring, due to intensive biomass burning there, associated with southwesterly wind [11,41–43].

Surface BrC concentrations also show a clear seasonality, with a maximum in winter (5.1 µg m^{-3}), followed by spring (2.8 µg m^{-3}), autumn (2.3 µg m^{-3}), and summer (1.3 µg m^{-3}). The high concentrations in winter are mainly due to the increasing residential combustion for heating, which could be confirmed by the largest contribution from residential combustion (82%) in winter (Table 3). In spring, the contribution of residential combustion reaches its minimum (48%), while the contribution of open biomass burning reaches a maximum of 35% compared with the other seasons. The lowest concentrations in summer could be partly attributed to the lowest emissions from residential combustion occurring in that season.

Table 3. Seasonal mean contributions from residential combustion, vehicle exhaust, and open biomass burning to BrC concentrations and BrC AAOD in China.

Sources	Concentration (%)				AAOD (%)			
	Winter	Spring	Summer	Autumn	Winter	Spring	Summer	Autumn
Residential combustion	82	48	56	64	83	58	79	80
Vehicle exhaust	15	17	32	27	12	8.9	12	12
Open biomass burning	3.0	35	12	8.3	4.8	33	9.3	7.5

3.3. BrC Absorption in China

Simulated AAOD in GEOS-Chem includes the contribution from BrC, BC, and dust. To evaluate the model results for BrC, we also compared model AAOD at 365 nm (with and without the contribution of BrC) with observed AAOD at 440 nm from AERONET sites (level 2.0 daily data [44]). Due to a limited number of valid observations in the year of 2018, only the data from two AERONET sites in Beijing were utilized for the comparison (Figure 3). The comparison shows a better agreement between AERONET and model AAOD at both sites after including the absorption of BrC resulting in the normalized mean bias (NMB) decreasing from −30~−32% to 14~21%. The slight overestimations could be attributed to the difference in the wavelength as the absorption decreases with the wavelength. As a result, it is expected to be higher at 365 nm than at 440 nm. The correlation coefficient *r* is similar at Beijing site and increases from 0.56 to 0.64 at Beijing-CAMS site. Simulated contribution of BrC to total AAOD at 365 nm at the two sites is about 22%. The comparison implies the importance of considering BrC absorption with regard of the estimates of AAOD in China.
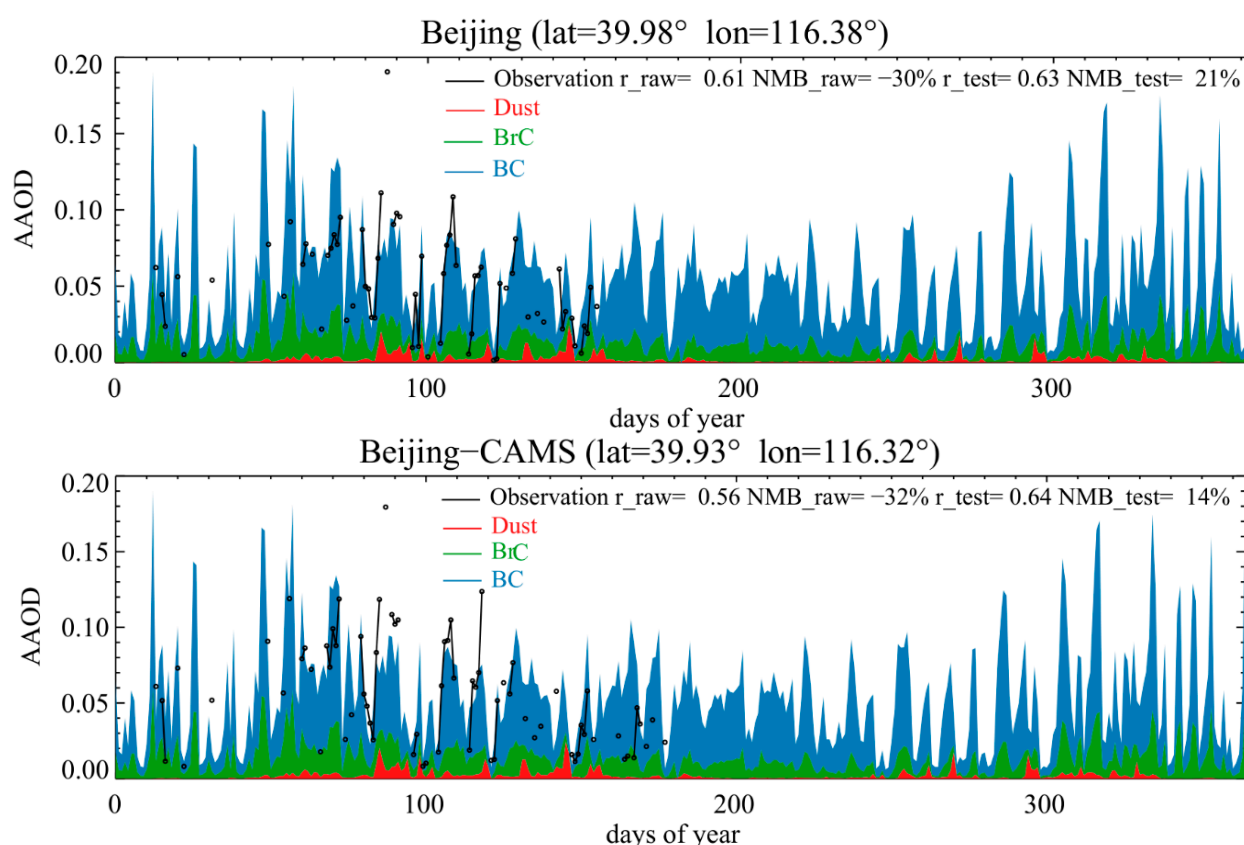
Figure 3. Time series of observed (black lines for AERONET) and simulated AAOD in 2018. Observations are from AERONET for 440 nm. Model results are for 365 nm and are further separated into BrC, BC, and dust. The correlation coefficients (r) and normalized mean bias (NMB) are also shown in the figure, where the suffix of 'raw' represents the results without BrC and the suffix of 'test' represents the result with BrC.

Figure 4 shows the simulated distribution of annual BrC AAOD at 365 nm in China in 2018, as well as the contributions from residential combustion, vehicle exhaust, and open biomass burning. Annual AAOD of BrC in China ranges from about 0.0017 to 0.060, with an average of 0.013. The distribution of AAOD is similar to surface concentrations, with higher values in Northeast Plain, North China Plain, and the Sichuan Basin (0.040–0.060). The contribution of residential combustion to BrC AAOD is the highest (73% on average), followed by vehicle exhausts (11%), and open biomass burning (16%). This is slightly different from the condition of surface BrC concentrations, which could largely be explained by the difference in the MAE among different sources. As listed in Table 2, BrC MAE from residential combustion (2.1 m^2 gC^{-1}) and open biomass burning (2.3 m^2 gC^{-1}) is much higher than the one from vehicle exhaust (0.74 m^2 gC^{-1}). This results in a relatively lower contribution from vehicle exhaust to BrC AAOD in comparison with the condition for BrC concentrations. North China and the Sichuan Basin are the areas with particularly high contributions from residential combustion (56–84%) and vehicle exhaust (~15%). The contributions of open biomass burning in most areas range from 3.0% to 15% but could reach up to 45% in the northeastern and southwestern border of China.
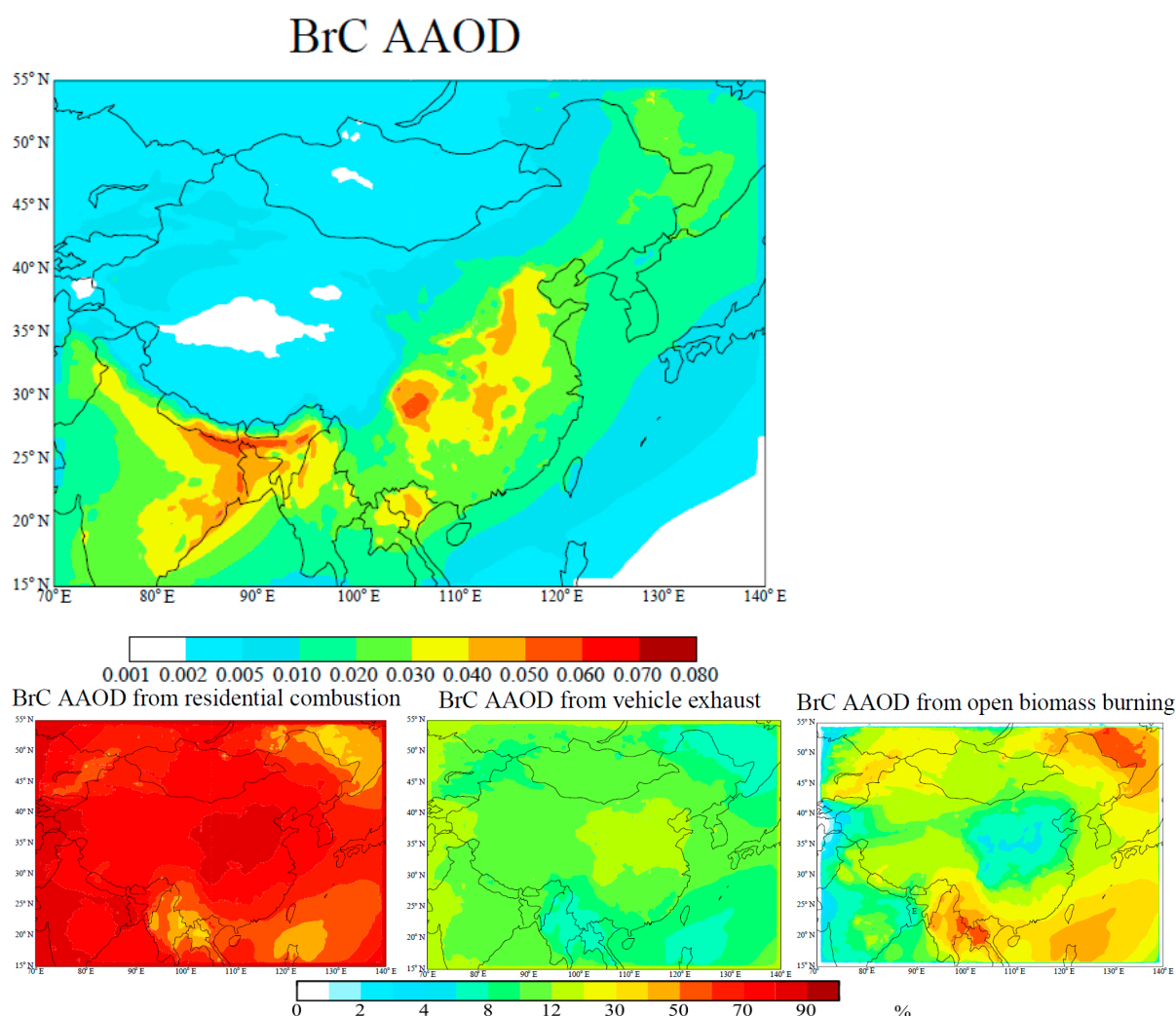
BrC AAOD

BrC AAOD from residential combustion   BrC AAOD from vehicle exhaust   BrC AAOD from open biomass burning

Figure 4. The spatial distribution of simulated annual BrC AAOD at 365 nm and the contribution from residential combustion, vehicle exhaust, and open biomass burning in 2018.

BrC AAOD also shows a clear seasonality with the maximum in spring (0.018), followed by winter (0.015), autumn (0.011), and summer (0.0091). The high value of AAOD in spring is probably associated with open biomass burning, which peaks in spring (33%) compared with the other seasons (Table 3). In addition, the BrC MAE for open biomass burning (2.3 m^2 gC^{-1}) is the highest among the three sources. In winter, the contribution of open biomass burning is the smallest (4.8%), while the contribution of residential combustion is the largest (83%).

Figure 5 also shows the contribution of BrC to the AAOD of carbonaceous aerosols at 365 nm in China. The contribution of BrC ranges from 45% to 67%, with an average of 52%. In contrast to the spatial distribution of BrC AAOD, the contribution of BrC to total carbonaceous aerosol AAOD is the smallest in North China and Sichuan Basin, where the contribution of vehicle exhaust is relatively high. High BrC contribution is generally found in areas that are more affected by open biomass burning. The results indicate that BrC and BC are of equal importance regarding the absorption at 365 nm, and thus the absorption due to BrC in China should not be ignored.
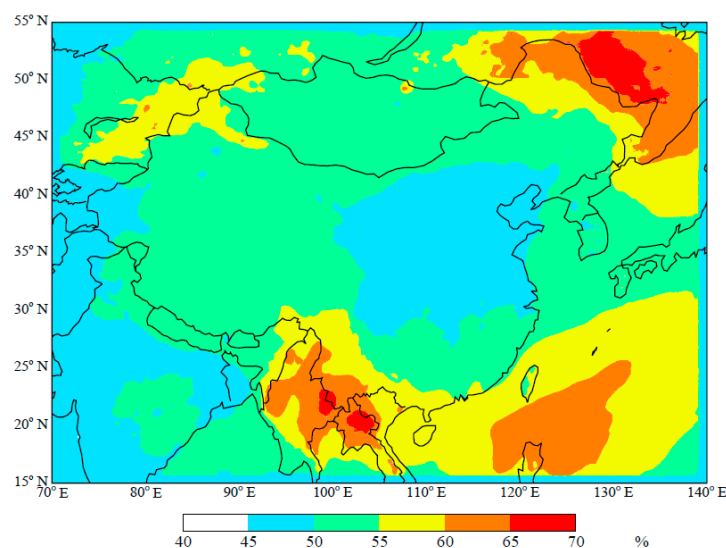
Figure 5. The contribution of BrC to total AAOD of carbonaceous aerosol (BC and BrC) at 365 nm in China in 2018.

4. Conclusions

BrC present in the atmosphere could not only degrade air quality, but also significantly contribute to global warming due to its absorption of solar radiation. Observations have shown high BrC concentrations and absorption in China, suggesting potentially large BrC emissions in China. However, previous modelling studies generally omit BrC or simply equate BrC with the OC emitted from biomass burning. In this study, we use the GEOS-Chem to simulate BrC distribution and its absorption in China, accounting for BrC emissions from residential coal and biofuel combustion, vehicle exhaust, and open biomass burning.

Based on the literature and related energy consumption data, we derive $E_{BrC/BC}$ of 3.9, 1.7, and 9.9 and MAE of 2.1 m^2 gC^{-1}, 0.74 m^2 gC^{-1}, and 2.3 m^2 gC^{-1} for BrC from residential combustion, vehicle exhaust, and open biomass burning, respectively. Combined with BC emissions, we estimate total BrC emissions of 3.42 Tg yr^{-1} in China in 2018, of which 71% is from residential combustion, 14% is from vehicle exhaust, and 15% is from open biomass burning. Surface BrC concentrations in China range from 0.050 μg m^{-3} to 20 μg m^{-3}, with higher values found in East and Central China than in West China. The major source of surface concentrations is residential combustion, accounting for 60%, on average, in China, followed by open biomass burning (23%) and vehicle exhaust emissions (17%). The surface BrC concentrations also show a clear seasonality, with the maximum in winter (5.1 μg m^{-3}), followed by spring (2.8 μg m^{-3}), autumn (2.3 μg m^{-3}), and summer (1.3 μg m^{-3}). The peak in winter is mainly because of the heating activity in that season.

The comparison with observed AAOD from two AERONET sites shows a significant improvement in the model results when the absorption of BrC is included, with NMB decreasing from −30~−32% to 14~21% and *r* increasing from 0.56 to 0.64. Annual BrC AAOD in Chian ranges from 0.0017 to 0.060 at 365 nm, with high values found in Northeast Plain, North China Plain, and the Sichuan Basin (0.040–0.060), mainly due to the contribution of residential combustion. The contribution of BrC to total carbonaceous aerosol AAOD at 365 nm ranges from 45% to 67%, indicating an equal importance of BrC and BC, and, therefore, the necessity of including BrC for accurate estimates of aerosol radiative forcing.

Author Contributions: Conceptualization, Q.W.; methodology, Q.W.; validation, Q.W.; formal analysis, Y.Z. and Q.W.; investigation, Y.Z., Q.W., X.Y., N.Y. and X.W.; data curation, Y.Z., Q.W., X.Y., N.Y. and X.W.; writing—original draft preparation, Y.Z.; writing—review and editing, Q.W.; visualization, Y.Z.; supervision, Q.W. All authors have read and agreed to the published version of the manuscript.

References

1. Andreae, M.O.; Gelencsér, A. Black carbon or brown carbon? The nature of light-absorbing carbonaceous aerosols. *Atmos. Chem. Phys.* **2006**, *6*, 3131–3148. [CrossRef]
2. Laskin, A.; Laskin, J.; Nizkorodov, S.A. Chemistry of atmospheric brown carbon. *Chem. Rev.* **2015**, *115*, 4335–4382. [CrossRef]
3. Moise, T.; Flores, J.M.; Rudich, Y. Optical properties of secondary organic aerosols and their changes by chemical processes. *Chem. Rev.* **2015**, *115*, 4400–4439. [CrossRef]
4. Chung, C.E.; Ramanathan, V.; Decremer, D. Observationally constrained estimates of carbonaceous aerosol radiative forcing. *Proc. Natl. Acad. Sci. USA* **2012**, *109*, 11624–11629. [CrossRef]
5. Feng, Y.; Ramanathan, V.; Kotamarthi, V.R. Brown carbon: A significant atmospheric absorber of solar radiation? *Atmos. Chem. Phys.* **2013**, *13*, 8607–8621. [CrossRef]
6. Saleh, R.; Robinson, E.S.; Tkacik, D.S.; Ahern, A.T.; Liu, S.; Aiken, A.C.; Sullivan, R.C.; Presto, A.A.; Dubey, M.K.; Yokelson, R.J.; et al. Brownness of organics in aerosols from biomass burning linked to their black carbon content. *Nat. Geosci.* **2014**, *7*, 647–650. [CrossRef]
7. Lin, G.; Penner, J.E.; Flanner, M.G.; Sillman, S.; Xu, L.; Zhou, C. Radiative forcing of organic aerosol in the atmosphere and on snow: Effects of SOA and brown carbon. *J. Geophys. Res. Atmos.* **2014**, *119*, 7453–7476. [CrossRef]
8. Alexander, D.T.L.; Crozier, P.A.; Anderson, J.R. Brown Carbon Spheres in East Asian Outflow and Their Optical Properties. *Science* **2008**, *321*, 833–836. [CrossRef] [PubMed]
9. Yan, J.; Wang, X.; Gong, P.; Wang, C.; Cong, Z. Review of brown carbon aerosols: Recent progress and perspectives. *Sci. Total Environ.* **2018**, *634*, 1475–1485. [CrossRef] [PubMed]
10. Zhang, Y.; Forrister, H.; Liu, J.; Dibb, J.; Anderson, B.; Schwarz, J.P.; Perring, A.E.; Jimenez, J.L.; Campuzano-Jost, P.; Wang, Y.; et al. Top-of-atmosphere radiative forcing affected by brown carbon in the upper troposphere. *Nat. Geosci.* **2017**, *10*, 486–489. [CrossRef]
11. Huang, L.; Lin, W.; Li, F.; Wang, Y.; Jiang, B. Climate Impacts of the Biomass Burning in Indochina on Atmospheric Conditions over Southern China. *Aerosol Air Qual. Res.* **2019**, *9*, 2707–2720. [CrossRef]
12. Voliotis, A.; Prokeš, R.; Lammel, G.; Samara, C. New insights on humic-like substances associated with wintertime urban aerosols from central and southern Europe: Size-resolved chemical characterization and optical properties. *Atmos. Environ.* **2017**, *166*, 286–299. [CrossRef]
13. Cheng, Y.; He, K.-b.; Du, Z.-y.; Engling, G.; Liu, J.-m.; Ma, Y.-l.; Zheng, M.; Weber, R.J. The characteristics of brown carbon aerosol during winter in Beijing. *Atmos. Environ.* **2016**, *127*, 355–364. [CrossRef]
14. Huang, R.J.; Yang, L.; Shen, J.; Yuan, W.; Gong, Y.; Guo, J.; Cao, W.; Duan, J.; Ni, H.; Zhu, C.; et al. Water-Insoluble Organics Dominate Brown Carbon in Wintertime Urban Aerosol of China: Chemical Characteristics and Optical Properties. *Environ. Sci. Technol.* **2020**, *54*, 7836–7847. [CrossRef] [PubMed]
15. Wang, L.; Li, Z.; Tian, Q.; Ma, Y.; Zhang, F.; Zhang, Y.; Li, D.; Li, K.; Li, L. Estimate of aerosol absorbing components of black carbon, brown carbon, and dust from ground-based remote sensing data of sun-sky radiometers. *J. Geophys. Res. Atmos.* **2013**, *118*, 6534–6543. [CrossRef]
16. Cheng, Y.; He, K.B.; Zheng, M.; Duan, F.K.; Ma, Y.L.; Du, Z.Y.; Tan, J.H.; Yang, F.M.; Liu, J.M.; Zhang, X.L.; et al. Mass absorption efficiency of elemental carbon and water-soluble organic carbon in Beijing, China. *Atmos. Chem. Phys. Discuss.* **2011**, *11*, 24727–24764.

17. Hecobian, A.; Zhang, X.; Zheng, M.; Frank, N.; Edgerton, E.S.; Weber, R.J. Water-Soluble Organic Aerosol material and the light-absorption characteristics of aqueous extracts measured over the Southeastern United States. *Atmos. Chem. Phys.* **2010**, *10*, 5965–5977. [CrossRef]

18. Du, Z.; He, K.; Cheng, Y.; Duan, F.; Ma, Y.; Liu, J.; Zhang, X.; Zheng, M.; Weber, R. A yearlong study of water-soluble organic carbon in Beijing II: Light absorption properties. *Atmos. Environ.* **2014**, *89*, 235–241. [CrossRef]

19. Zhai, X.; Cao, F.; Zhang, S.; Yang, X.; Zhang, Y. Contribution of biomass burning on light absorption property of water soluble organic carbon in PM 2.5 in Sanjiang Plain, Northeast China. *Ecol. Environ. Sci.* **2019**, *28*, 523–530. (In Chinese)

20. Liu, J.; Bergin, M.; Guo, H.; King, L.; Kotra, N.; Edgerton, E.; Weber, R.J. Size-resolved measurements of brown carbon in water and methanol extracts and estimates of their contribution to ambient fine-particle light absorption. *Atmos. Chem. Phys.* **2013**, *13*, 12389–12404. [CrossRef]

21. Park, S.; Yu, G.-H.; Lee, S. Optical absorption characteristics of brown carbon aerosols during the KORUS-AQ campaign at an urban site. *Atmos. Res.* **2018**, *203*, 16–27. [CrossRef]

22. Chakrabarty, R.K.; Moosmüller, H.; Chen, L.W.A.; Lewis, K.; Arnott, W.P.; Mazzoleni, C.; Dubey, M.K.; Wold, C.E.; Hao, W.M.; Kreidenweis, S.M. Brown carbon in tar balls from smoldering biomass combustion. *Atmos. Chem. Phys.* **2010**, *10*, 6363–6370. [CrossRef]

23. Xie, M.; Hays, M.D.; Holder, A.L. Light-absorbing organic carbon from prescribed and laboratory biomass burning and gasoline vehicle emissions. *Sci. Rep.* **2017**, *7*, 7318. [CrossRef] [PubMed]

24. Lack, D.A.; Langridge, J.M.; Bahreini, R.; Cappa, C.D.; Middlebrook, A.M.; Schwarz, J.P. Brown carbon and internal mixing in biomass burning particles. *Proc. Natl. Acad. Sci. USA* **2012**, *109*, 14802–14807. [CrossRef]

25. Sun, J.; Zhi, G.; Hitzenberger, R.; Chen, Y.; Tian, C.; Zhang, Y.; Feng, Y.; Cheng, M.; Zhang, Y.; Cai, J.; et al. Emission factors and light absorption properties of brown carbon from household coal combustion in China. *Atmos. Chem. Phys.* **2017**, *17*, 4769–4780. [CrossRef]

26. Wang, Q.; Saturno, J.; Chi, X.; Walter, D.; Lavric, J.V.; Moran-Zuloaga, D.; Ditas, F.; Pöhlker, C.; Brito, J.; Carbone, S.; et al. Modeling investigation of light-absorbing aerosols in the Amazon Basin during the wet season. *Atmos. Chem. Phys.* **2016**, *16*, 14775–14794. [CrossRef]

27. Saleh, R.; Marks, M.; Heo, J.; Adams, P.J.; Donahue, N.M.; Robinson, A.L. Contribution of brown carbon and lensing to the direct radiative effect of carbonaceous aerosols from biomass and biofuel burning emissions. *J. Geophys. Res. Atmos.* **2015**, *120*, 10–285. [CrossRef]

28. Cai, J.; Zhi, G.; Chen, Y.; Meng, F.; Xue, Z.; Li, J.; Fang, Y. A Preliminary Study on Brown Carbon Emissions from Open Agricultural Biomass Burning and Residential Coal Combustion in China (in Chinese). *Res. Environ. Sci.* **2014**, *27*, 455–461.

29. Lucchesi, R.; File Specification for GEOS-FP. GMAO Office Note No. 4 (Version 1.2) 2018; p. 61. Available online: http://gmao.gsfc.nasa.gov/pubs/office_notes (accessed on 2 May 2021).

30. Park, R.J.; Jacob, D.J.; Chin, M.; Martin, R.V. Sources of carbonaceous aerosols over the United States and implications for natural visibility. *J. Geophys. Res.* **2003**, *108*. [CrossRef]

31. Koster, R.; Darmenov, A.; Silva, A. *The Quick Fire Emissions Dataset (QFED): Documentation of Versions 2.1, 2.2 and 2.4*; Technical Report Series on Global Modeling and Data Assimilation; NASA: Washington, DC, USA, 2015; Volume 38.

32. Sun, J.; Zhang, Y.; Zhi, G.; Hitzenberger, R.; Jin, W.; Chen, Y.; Wang, L.; Tian, C.; Li, Z.; Chen, R.; et al. Brown carbon's emission factors and optical characteristics in household biomass burning: Developing a novel algorithm for estimating the contribution of brown carbon. *Atmos. Chem. Phys.* **2021**, *21*, 2329–2341. [CrossRef]

33. Wang, R.; Tao, S.; Wang, W.; Liu, J.; Shen, H.; Shen, G.; Wang, B.; Liu, X.; Li, W.; Huang, Y.; et al. Black carbon emissions in China from 1949 to 2050. *Environ. Sci. Technol.* **2012**, *46*, 7595–7603. [CrossRef]

34. Tang, J.; Li, J.; Su, T.; Han, Y.; Mo, Y.; Jiang, H.; Cui, M.; Jiang, B.; Chen, Y.; Tang, J.; et al. Molecular compositions and optical properties of dissolved brown carbon in biomass burning, coal combustion, and vehicle emission aerosols illuminated by excitation–emission matrix spectroscopy and Fourier transform ion cyclotron resonance mass spectrometry analysis. *Atmos. Chem. Phys.* **2020**, *20*, 2513–2532.

35. Li, M.; Fan, X.; Zhu, M.; Zou, C.; Song, J.; Wei, S.; Jia, W.; Peng, P. Abundance and Light Absorption Properties of Brown Carbon Emitted from Residential Coal Combustion in China. *Environ. Sci. Technol.* **2019**, *53*, 595–603. [CrossRef] [PubMed]

36. Wang, Y.; Wang, Y.; Song, S.; Wang, T.; Li, D.; Tan, H. Effects of coal types and combustion conditions on carbonaceous aerosols in flue gas and their light absorption properties. *Fuel* **2020**, *277*, 118148. [CrossRef]

37. Pani, S.K.; Lin, N.H.; Griffith, S.M.; Chantara, S.; Lee, C.T.; Thepnuan, D.; Tsai, Y.I. Brown carbon light absorption over an urban environment in northern peninsular Southeast Asia. *Environ. Pollut.* **2021**, *276*, 116735. [CrossRef]

38. Zhang, Y.; Peng, Y.; Song, W.; Zhang, Y.-L.; Ponsawansong, P.; Prapamontol, T.; Wang, Y. Contribution of brown carbon to the light absorption and radiative effect of carbonaceous aerosols from biomass burning emissions in Chiang Mai, Thailand. *Atmos. Environ.* **2021**, 118544. [CrossRef]

39. Zhang, A.; Wang, Y.; Zhang, Y.; Weber, R.J.; Song, Y.; Ke, Z.; Zou, Y. Modeling the global radiative effect of brown carbon: A potentially larger heating source in the tropical free troposphere than black carbon. *Atmos. Chem. Phys.* **2020**, *20*, 1901–1920. [CrossRef]

40. Yang, M.; Howell, S.G.; Zhuang, J.; Huebert, B.J. Attribution of aerosol light absorption to black carbon, brown carbon, and dust in China—Interpretations of atmospheric measurements during EAST-AIRE. *Atmos. Chem. Phys.* **2009**, *9*, 2035–2050. [CrossRef]

41. Liang, Y.; Gui, K.; Zheng, Y.; Yang, X.; Li, X.; Liu, C.; Sheng, Z.; Sun, T.; Zhang, X.; Che, H. Impact of Biomass Burning in South and Southeast Asia on Background Aerosol in Southwest China. *Aerosol Air Qual. Res.* **2019**, *19*, 1188–1204. [CrossRef]
42. Zheng, L.; Yang, X.; Lai, S.; Ren, H.; Yue, S.; Zhang, Y.; Huang, X.; Gao, Y.; Sun, Y.; Wang, Z.; et al. Impacts of springtime biomass burning in the northern Southeast Asia on marine organic aerosols over the Gulf of Tonkin, China. *Environ. Pollut.* **2018**, *237*, 285–297. [CrossRef] [PubMed]
43. Xin, Y.; Wang, G.; Chen, L. Identification of Long-Range Transport Pathways and Potential Sources of PM10 in Tibetan Plateau Uplift Area: Case Study of Xining, China in 2014. *Aerosol Air Qual. Res.* **2016**, *16*, 1044–1054. [CrossRef]
44. Dubovik, O.; Holben, B.; Eck, T.F.; Smirnov, A.; Kaufman, Y.; King, M.; Tanré, D.; Slutsker, I. Variability of Absorption and Optical Properties of Key Aerosol Types Observed in Worldwide Locations. *J. Atmos. Sci.* **2002**, *59*, 590–608. [CrossRef]